



ELSEVIER

Contents lists available at ScienceDirect

Journal of Luminescence

journal homepage: www.elsevier.com/locate/jlumin

CeF₃/TiO₂ composite as a novel visible-light-driven photocatalyst based on upconversion emission and its application for photocatalytic reduction of CO₂



Chunni Tang^{a,b}, Wenqian Hou^a, Enzhou Liu^a, Xiaoyun Hu^c, Jun Fan^{a,*}

^a School of Chemical Engineering, Northwest University, Xi'an 710069, PR China

^b Department of Chemical Engineering, Shaanxi Institute of Technology, Xi'an 710300, PR China

^c Department of Physics, Northwest University, Xi'an 710069, PR China

ARTICLE INFO

Article history:

Received 18 January 2014

Received in revised form

25 April 2014

Accepted 28 April 2014

Available online 13 May 2014

Keywords:

Photocatalytic Reduction Of Co₂

Upconversion Luminescence

CeF₃

TiO₂

ABSTRACT

Novel upconversion luminescent material CeF₃ and visible-light-driven photocatalyst CeF₃/TiO₂ composite were synthesized by microwave-hydrothermal method and microwave-alcoholthermal method respectively. The prepared samples were characterized by XRD, TEM, SEM, EBSD, EDS and PL. The CeF₃/TiO₂ composite was applied on the photocatalytic reduction of CO₂ with H₂O under visible light irradiation (> 515 nm). XRD and TEM images showed that the as-prepared CeF₃ sample was hexagonal phase and hollow sphere-like or rod-like nanocrystal. The study of fluorescent spectrum indicated that CeF₃ could convert visible light (420–600 nm) into ultraviolet light (285–380 nm), and two emission peaks at 304 nm and 324 nm were observed under the excitation of 524 nm and 554 nm at room temperature. XRD, SEM, EBSD and EDS images indicated that CeF₃ particles were well wrapped or intermixed with TiO₂ particles in the CeF₃/TiO₂ composite. The results showed that CeF₃/TiO₂ was an effective photocatalyst for CO₂ reduction under visible light than pure TiO₂ due to the upconversion emission; the corresponding average energy efficiencies were about 0.2% and 0%, and methanol yields were 162.2 and 0 μmol/g-cat under the same conditions. Additionally, the mechanism of photocatalytic reduction of CO₂ on CeF₃/TiO₂ composite was proposed.

© 2014 Elsevier B.V. All rights reserved.

1. Introduction

Over the past decades, the increasing in the level of atmospheric carbon dioxide (CO₂) due to fossil fuel combustion has raised serious concerns about global warming, and it is extremely urgent to study the conversion and utilization of CO₂. CO₂ itself is a kind of potential carbon resource, and it can be converted into fuels, such as CH₄, CH₃OH, CO and low carbon hydrocarbons [1–3], which is helpful not only to eliminate the atmospheric greenhouse effect, but also to synthesize organic fuels or chemical intermediates and save fossil resources such as oil, natural gas and coal. At present, since solar energy and H₂O are clean, abundant and non-polluting, research studies are focusing on the solar photocatalytic reduction of CO₂ with H₂O into hydrocarbon fuels by photocatalysts [4,5], which has the potential to store intermittent solar energy and to recycle CO₂.

Titania (TiO₂) has been extensively studied as a photocatalyst for applications such as water and air remediation, hydrogen evolution and photocatalytic reduction of CO₂ [6–9], because of its relatively high reactivity, physical and chemical stability. However, TiO₂ has a relatively large band gap (3.2 eV) that requires ultraviolet (UV) light (< 387 nm, about 5% of the solar spectrum) for activation. Therefore, it is of interest to develop a TiO₂-based photocatalyst which is sensitive to visible light (about 48% of the solar spectrum) in order to make more efficient use of solar energy in practical applications. Various strategies have been employed including doping metal or nonmetal elements, surface photosensitization and combination with narrow band gap semiconductors [10–12].

Recently, much attention has been paid to extending the photoresponse range of TiO₂ by upconversion luminescent material (ULM) including Y₃Al₅O₁₂:Er³⁺, Y₂O₃:Er³⁺, YAlO₃:Er³⁺, NaYF₄:Er³⁺, 40CdF₂·60BaF₂·xEr₂O₃ and 10BaF₂:NaF, Na₃Al₆ [13–19]. Rare-earth CeF₃ exhibits good luminescence property, lower phonon-energy, and special lamellar structure. Therefore, it is regarded as a most promising candidate for the materials in high-energy physics, biomarker, and lubricant [20–22]. However,

* Corresponding author. Tel.: +86 29 8800 2223; fax: +86 29 8830 5252.

E-mail address: fanjun@nwu.edu.cn (J. Fan).

CeF₃ was rarely considered as an ULM in the past years because energy levels of Ce³⁺ are too simple and lack of corresponding metastable energy levels in the visible region or near infrared region. Recently, it was demonstrated that the upconversion luminescence of Ce³⁺ doped in different host materials excited by simultaneous absorption of three infrared photons using the femtosecond laser irradiation [23–25]. This discovery suggests that Ce³⁺ doped materials can be good candidates for ULM. Compared with other host materials, fluoride is an excellent ground host material, so CeF₃ may be a promising ULM.

To the best of our knowledge, there is rare study on the upconversion fluorescence properties of CeF₃, the synthesis and application of CeF₃/TiO₂ composite. In this paper, the CeF₃ was prepared and its upconversion luminescence properties were investigated. Subsequently, a visible-light-driven composite photocatalyst (CeF₃/TiO₂) was prepared, its photocatalytic activity was tested and the mechanism was proposed as well. The photocatalytic reduction of CO₂ under visible light irradiation was found to be effective.

2. Experiments

2.1. Preparation of CeF₃

The CeF₃ sample was prepared by a microwave-hydrothermal method. NH₄F aqueous solution (0.067 M) was dripped into the Ce(NO₃)₃ aqueous solution (0.6 M) under stirring. After stirring for 30 min, the suspension was transferred into a Teflon-lined vessel and experienced a microwave treatment. Finally, the product was collected by centrifugation and washed with distilled water and ethanol for several times, and dried at 60 °C.

2.2. Preparation of CeF₃/TiO₂ composite

A microwave-alcoholothermal method was employed to synthesize the CeF₃/TiO₂ composite. 0.4 g CeF₃ was dispersed in ethanol and injected with 7.8 mL acetic acid. Then, 6.6 mL butyl titanate dispersed in ethanol was added to the suspension with a controlling speed upon stirring. After stirring for 30 min, the above precursor suspension experienced a microwave treatment (180 °C, 600 W, 30 min), centrifugation, washing and drying. The dry powder was annealed to obtain the CeF₃/TiO₂ composite. In addition, pure TiO₂ was fabricated by the same method without addition of CeF₃ to be a reference.

2.3. Characterization

X-ray diffraction patterns (XRD) of the samples were obtained on a Bruker D8 Advance Diffractometer with high intensity Cu K_{α1} (λ=0.15406 nm). Field-emission scanning electron microscope (SEM) images were taken on a JSM-6390A electron microscope with electron backscattered diffraction (EBSD) and energy-dispersive X-ray (EDS). Transmission electron microscope (TEM) images were recorded on a JEM-100SX electron microscope. Room temperature upconversion luminescence properties were observed using a fluorescence spectrophotometer (Hitachi F-7000).

2.4. Visible light photocatalytic tests

Visible light photocatalytic tests were evaluated by photocatalytic reduction of CO₂ with H₂O in a circulated quartz photoreactor. A spherical xenon lamp (500 W) with sun-like radiation spectrum equipped with a 515-nm cutoff optical filter was employed as the visible light source of the self-made reactor. The system was shielded by a black box during the reaction to prevent the reactor

from being interfered with outside light. In a typical experiment, 0.4 g of photocatalyst was suspended in 400 mL of distilled water. Prior to irradiation, CO₂ (99.995%) was bubbled through the reactor for at least 30 min to eliminate dissolved oxygen and saturate the solution. The concentrations of reduction product of CH₃OH were monitored using a GC9790 gas chromatography. The methanol yield and energy efficiency were calculated based on Eqs. (1) and (2) below.

$$Y_{\text{CH}_3\text{OH}} = (C_{\text{CH}_3\text{OH}} \times V_{\text{rea}}) / M_{\text{cat}} \quad (1)$$

$$E_e = \Delta H_{\text{CH}_3\text{OH}} (C_{\text{CH}_3\text{OH}} \times V_{\text{rea}}) / E_a \quad (2)$$

where $Y_{\text{CH}_3\text{OH}}$ is the methanol yield, in micromoles per gram of catalyst, $C_{\text{CH}_3\text{OH}}$ is the methanol concentration, in micromoles per liter, V_{rea} is the volume of reaction solution, in liter, M_{cat} is the mass of the photocatalyst, in gram, E_e is the energy efficiency, $\Delta H_{\text{CH}_3\text{OH}}$ is the combustion heat of methanol, in joules per mole, E_a is the energy of photons absorbed by photocatalyst, in joule

3. Results and discussion

3.1. Microstructure analysis

Fig. 1 shows the XRD patterns of the as-synthesized CeF₃, TiO₂ and CeF₃/TiO₂ composite. The high and sharp peaks in the patterns indicate that all of the samples are well crystallized. The characteristic diffraction peaks of the hexagonal phase CeF₃ and anatase TiO₂ can be observed in the XRD patterns of CeF₃ and TiO₂ samples, which are in good agreement with those in the standard JCPDS file nos. 08-0045 and 21-1272 respectively. The pattern of CeF₃/TiO₂ composite includes both characteristic diffraction peaks of the hexagonal phase CeF₃ and anatase TiO₂ without other impurity peaks, which indicates that the composite process does not change the crystalline phase and chemical properties of TiO₂ and CeF₃.

The sizes and morphology of the as-prepared CeF₃, TiO₂ and CeF₃/TiO₂ composite are investigated in Fig. 2. As shown in Fig. 2 (a), the CeF₃ samples are nano hollow sphere-like or rod-like particles. The sphere-like nanoparticles have a diameter of about 15–35 nm, while the rod-like nanoparticles have a length of about 20–30 nm and a diameter of about 15 nm. It is apparent that the CeF₃ samples consist of a large number of nanoparticles with a relatively uniform size which tends to adhere to each other (Fig. 2 (b)). However, in the SEM and EBSD images of CeF₃/TiO₂ composite (Fig. 2(c) and (d)), very few CeF₃ nanoparticles are found on the surface of the TiO₂ particles or between the TiO₂ particles, which indicates that CeF₃ particles are well wrapped or intermixed with TiO₂ particles. The EDS image of CeF₃/TiO₂ composite is used to

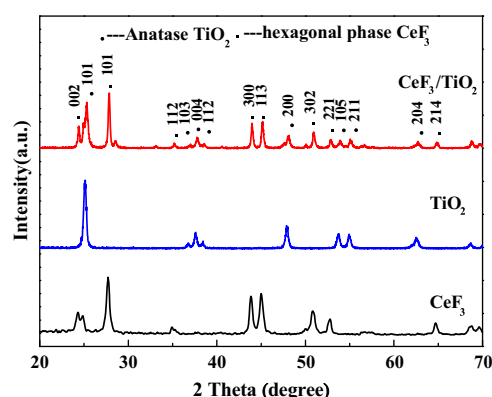


Fig. 1. XRD patterns of CeF₃, TiO₂ and CeF₃/TiO₂ composite.

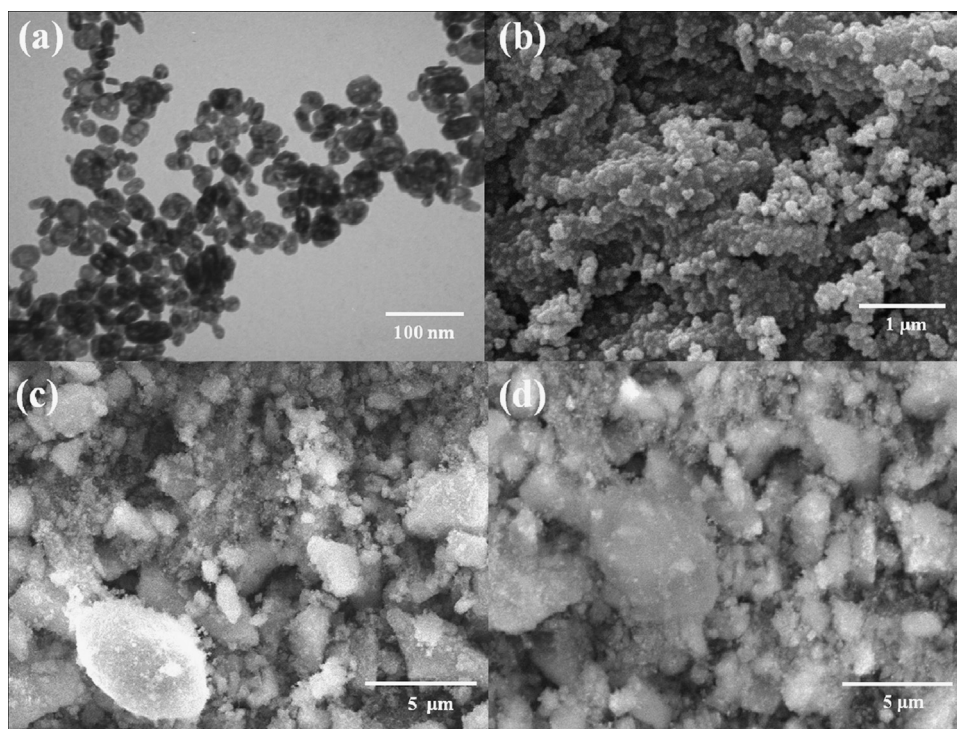


Fig. 2. TEM image of (a) CeF_3 , SEM images of (b) CeF_3 and (c) $\text{CeF}_3/\text{TiO}_2$, EBSD image of (d) $\text{CeF}_3/\text{TiO}_2$.

analyze element composition, and the result is shown in Fig. 3. Ti, O, Ce and F are obviously found in the spectrum, confirming the existence of CeF_3 and TiO_2 in the $\text{CeF}_3/\text{TiO}_2$ composite.

3.2. Upconversion luminescence properties

The three-dimensional upconversion luminescence scan spectrum of CeF_3 was measured (seen in Fig. 4). It can be seen clearly that the visible light (420–600 nm) can be effectively converted into ultraviolet (UV) light (285–380 nm) by CeF_3 . Fig. 5 shows the upconversion luminescence emission and excitation spectra of CeF_3 . Using the monitoring wavelengths at 524 nm and 554 nm respectively, two UV emission peaks at 304 nm and 324 nm are detected in the emission spectrum of CeF_3 (Fig. 5(a) and (b)). Using the monitoring wavelength at 324 nm, two visible light excitation peaks at 524 nm and 554 nm are found in the excitation spectrum of CeF_3 (Fig. 5(c)).

Further investigations revealed that CeF_3 can also emit two emission peaks at 304 nm and 324 nm when it is excited by 260 nm and 280 nm (seen in Fig. S1 in Supporting information). This downconversion luminescence is probably assigned to Ce^{3+} electrons' transfer between the different sub-levels of 5d excited states split by the crystal field [26] and the 4f ground state ($^2F_{5/2}$ and $^2F_{7/2}$). The phenomenon demonstrates obvious properties of broad-band absorption and emission, which is in consistency with most references [27–29]. It is apparent that the emission peaks of upconversion luminescence are similar to that of the downconversion luminescence in shapes and positions, which indicates that they undergo a similar emission process. The excitation energy of 260 nm is almost twice as much as the excitation energy of 524 nm. Meanwhile, the excitation energy of 280 nm is almost twice as much as the excitation energy 554 nm. Therefore, the upconversion of visible light is dominated by a two-photon excitation process. However, because there are no intermediate energy levels between 5d and 4f levels of Ce^{3+} , it may be deduced to a multi-photon simultaneous absorption. This mechanism could be considered that more than one photon are absorbed at the

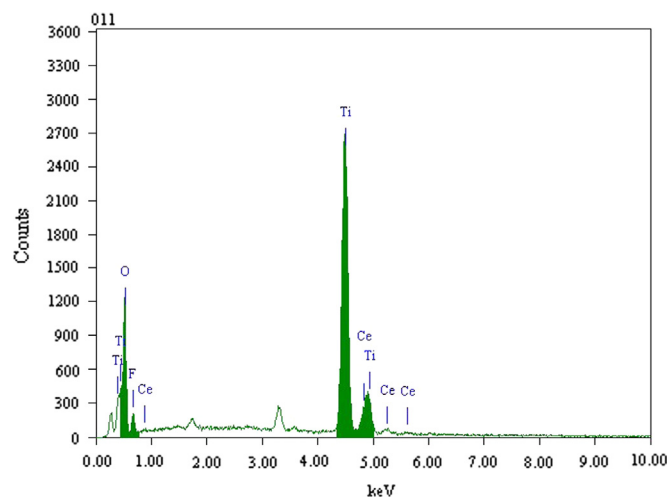


Fig. 3. EDS image of $\text{CeF}_3/\text{TiO}_2$ composite.

same time, which results in direct electron excitation from an initial state to a final state.

The possible luminescence process of CeF_3 is showed Fig. S2 in supporting information. First, an electron located on the ground state ($^2F_{5/2}$) absorbs one 260 nm photon (4.77 eV) or simultaneously absorbs two 524 nm photons (2.37 eV) and transfer to the excited 5d state (4.77 eV); it absorbs one 280 nm photon (4.43 eV) or simultaneously absorbs two 554 nm photons (2.24 eV) and transfer to the excited 5d state (4.43 eV). Then, the electron nonradiatively relaxes to the lowest 5d state (4.08 eV). Finally, the transitions from the lowest 5d state to the ground state ($^2F_{5/2}$) or the state ($^2F_{7/2}$) result in the emission peaks at 304 nm and 324 nm.

3.3. Photocatalytic properties

The visible light photocatalytic properties of $\text{CeF}_3/\text{TiO}_2$ composite were measured by photocatalytic reduction of CO_2 with H_2O

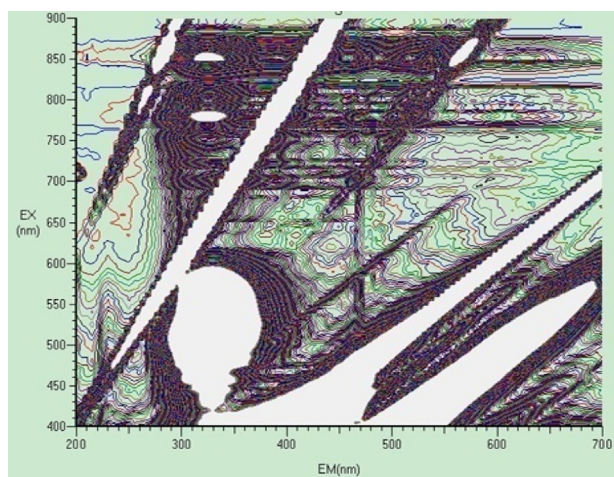


Fig. 4. The three-dimensional upconversion luminescence scan spectrum of CeF_3 .

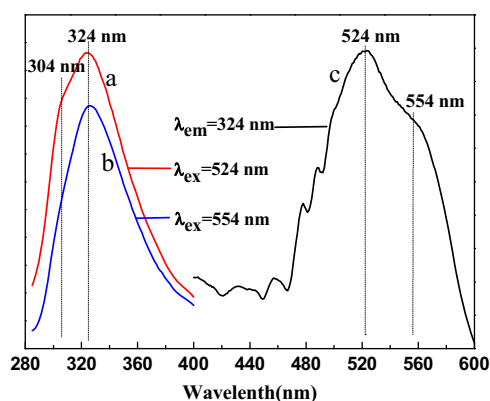


Fig. 5. Upconversion luminescence emission spectra of CeF_3 (a and b), excitation luminescence spectrum of CeF_3 (c).

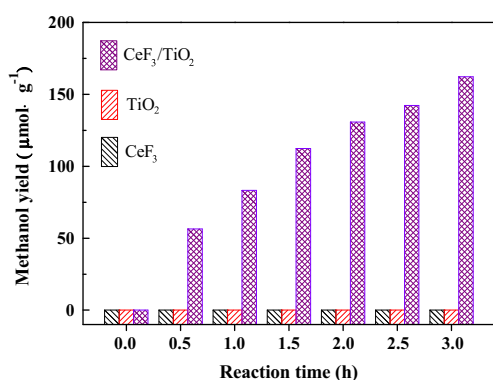


Fig. 6. Methanol yields of photocatalytic reaction of CO_2 under visible light irradiation ($\lambda > 515 \text{ nm}$) using the TiO_2 , CeF_3 and $\text{TiO}_2/\text{CeF}_3$ as catalysts respectively.

with the irradiation of visible light ($\lambda > 515 \text{ nm}$). Fig. 6 shows that $\text{CeF}_3/\text{TiO}_2$ composite has obviously effective activity, and the corresponding methanol yield fleetly increases at the beginning and reaches its maximum ($162.2 \mu\text{mol}/\text{g}\text{-cat}$) at 3.0 h. Meanwhile, the average energy efficiency was about 0.2% on the $\text{CeF}_3/\text{TiO}_2$ composite in 3.0 h. However, pure TiO_2 and CeF_3 do not show any photocatalytic activity when used separately under the same conditions. The result illustrates that the visible light ($\lambda > 515 \text{ nm}$) catalytic activity of TiO_2 can be initiated under the existence of CeF_3 , which is because TiO_2 can absorb the UV light converted from visible light by CeF_3 .

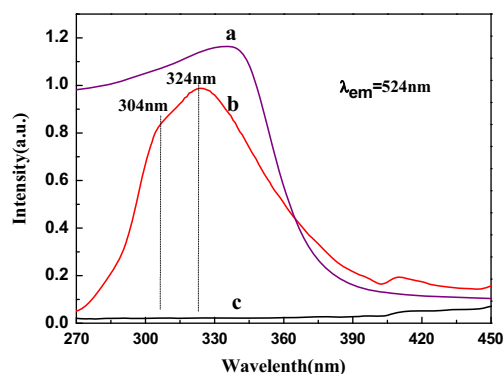


Fig. 7. Absorption spectrum of TiO_2 (a), upconversion emission spectrum of CeF_3 (b), and upconversion emission spectrum of $\text{CeF}_3/\text{TiO}_2$ (c).

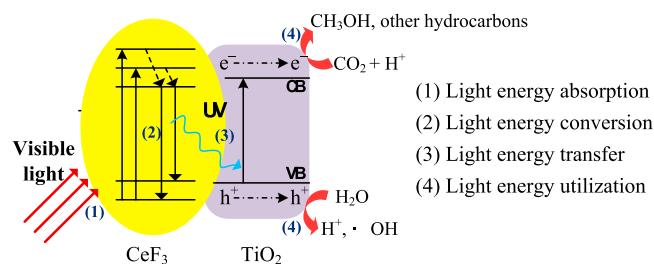
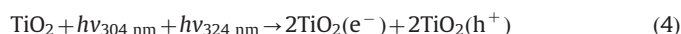
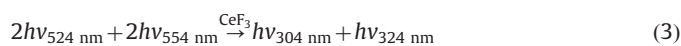


Fig. 8. Mechanism of photocatalytic reduction of CO_2 on $\text{TiO}_2/\text{CeF}_3$.

3.4. Mechanism of photocatalytic reduction of CO_2

The visible-light-driven photocatalysis based on upconversion emission depends on the energy transfer from CeF_3 to TiO_2 . The requirement for an efficient energy transfer is to make the donor (CeF_3) emission band overlap with the absorption band of the acceptor (TiO_2). The upconversion emission spectrum of CeF_3 and the absorption spectrum of TiO_2 are presented in Fig. 7. It is very clear that the absorption band of TiO_2 (Fig. 7(a)) overlaps very well with the UV emission of CeF_3 particles (Fig. 7(b)). To examine this energy transfer process, the upconversion emission spectra of $\text{CeF}_3/\text{TiO}_2$ was recorded under the excitation of 524 nm (Fig. 7 (c)). The intensities of UV emission peaks are immensely reduced after the combination of TiO_2 , which indicates effective energy transfer between CeF_3 and TiO_2 . The comparison of the visible light photocatalytic activities between the donor and acceptor and the donor-acceptor pairs could provide direct evidences for the energy transfer (refer Section 3.3).

The mechanism [30] of photocatalytic reduction of CO_2 on $\text{TiO}_2/\text{CeF}_3$ is shown in Fig. 8. Firstly, the incident visible light was absorbed by CeF_3 . Secondly, the visible light was converted into UV light by CeF_3 . Subsequently, the UV light is absorbed by TiO_2 particles, and electron (e^-)-hole (h^+) pairs are formed and located in the conduction band and valence band of TiO_2 . Finally, redox reactions are initiated by e^- and h^+ on the surface of TiO_2 . The active h^+ can oxidize H_2O to form hydroxyl radicals ($\text{OH}\cdot$) which could release O_2 and H^+ . H^+ and high active e^- will facilitate CO_2 reduction and produce methanol or other hydrocarbons. It indicates that six electrons are required to convert CO_2 into CH_3OH . It is apparent that CeF_3 plays a crucial role in the above process.



4. Conclusions

CeF₃ hollow nanostructures with upconversion luminescence properties was synthesized by a microwave-hydrothermal method, and TiO₂/CeF₃ composite was prepared as a visible-light-driven photocatalyst based on upconversion emission by a microwave-alcoholthermal method. The microstructures, properties and mechanism of upconversion luminescence of the resulting samples were investigated. The energy transfer from CeF₃ to TiO₂ under visible light irradiation was confirmed. The visible light driven photocatalysis was realized by photocatalytic reduction of CO₂ with H₂O. This study suggested a promising method to develop the visible light driven photocatalyst, which may have a profound implication on the future utilization of solar energy and recycling CO₂.

Acknowledgments

This work was supported by the National Natural Science Foundation of China (Nos. 21306150, 21176199 and 51372201), the Specialized Research Fund for the Doctoral Program of Higher Education of China (No. 20136101110009), the Shaanxi Provincial Research Foundation for Basic Research, China (No. 2013JQ2003), the Scientific Research and Industrialization Cultivation Foundations of Education Department of Shaanxi Provincial Government, China (Nos. 2013JK0693 and 2011JG05), the Scientific Research Foundation of Northwest University (No. 12NW19), and the Scientific Research Starting Foundation of Northwest University (No. PR12216).

Appendix A. Supporting information

Supplementary data associated with this article can be found in the online version at <http://dx.doi.org/10.1016/j.jlumin.2014.04.040>.

References

- [1] S.C. Roy, O.K. Varghese, M. Paulose, C.A. Grimes, *ACS Nano* 4 (2010) 1259.
- [2] O.K. Varghese, M. Paulose, T.J. LaTempa, C.A. Grimes, *Nano Lett.* 9 (2009) 731.
- [3] H.Q. Sun, S.B. Wang, *Energy Fuels* 28 (2014) 22.
- [4] V.P. Indrakanti, H.H. Schobert, J.D. Kubicki, *Energy Fuels* 23 (2009) 5247.
- [5] Y.G. Wang, F. Wang, Y.T. Chen, D.F. Zhang, B. Li, S.F. Kang, X. Li, L.F. Cui, *Appl. Catal. B* 147 (2014) 602.
- [6] Y. Kuwahara, J. Aoyama, K. Miyakubo, T. Eguchi, T. Kamegawa, K. Mori, H. Yamashit, *J. Catal.* 285 (2012) 223.
- [7] P. Wei, J.W. Liu, Z.H. Li, *Ceram. Int.* 39 (2013) 5387.
- [8] A. Galinska, J. Walendziewski, *Energy Fuels* 19 (2005) 1143.
- [9] M. Tahir, N.S. Amin, *Appl. Catal. A* 467 (2013) 483.
- [10] B. Srinivas, K. Lalitha, P.A.K. Reddy, G. Rajesh, V.D. Kumari, M. Subrahmanyam, B.R. De, *Res. Chem. Intermed.* 37 (2011) 1069.
- [11] N.R. Khalid, E. Ahmed, Z.L. Hong, Y.W. Zhang, M. Ullah, M. Ahmed, *Ceram. Int.* 39 (2013) 3569.
- [12] Y.H. Zheng, Y.N. Chen, C.Q. Yang, Q.M. Wang, J.T. Lin, L.G. Zhang, *J. Lumin.* 132 (2012) 1639.
- [13] L.N. Yin, Y. Li, J. Wang, Y. Zhai, Y.M. Kong, J.Q. Gao, G.X. Han, P. Fan, *J. Lumin.* 132 (2012) 3010.
- [14] Y.X. Ye, E.Z. Liu, X.Y. Hu, Z.Y. Yan, Z.Y. Jiang, J. Fan, *Chin. Sci. Bull.* 5 (2011) 2668.
- [15] J. Wang, Y.P. Xie, Z.H. Zhang, J. Li, C.W. Li, L.Q. Zhang, Z.Q. Xing, R. Xu, X. D. Zhang, *Environ. Chem. Lett.* 8 (2010) 87.
- [16] Y.X. Ye, X.Y. Hu, Z.Y. Yan, E.Z. Liu, J. Fan, D.K. Zhang, H. Miao, Y.B. Shang, J. Yang, *Chin. Phys. B* 20 (2011) 087803.
- [17] G.B. Shan, H. Assaaoudi, G.P. Demopoulos, *ACS Appl. Mater. Interfaces* 3 (2011) 3239.
- [18] J. Wang, T. Ma, G. Zhang, Z.H. Zhang, X.D. Zhang, Y.F. Jianga, G. Zhao, P. Zhang, *Catal. Commun.* 8 (2007) 607.
- [19] E.Z. Liu, J. Fan, X.Y. Hu, W.Q. Hou, H.Z. Dai, *Chin. Phys. B* 21 (2012) 3403.
- [20] Y. Pei, X. Chen, D. Yao, G. Ren, *Radiat. Meas.* 42 (2007) 1351.
- [21] C. Li, J. Yang, P. Yang, H. Lian, J. Lin, *Chem. Mater.* 20 (2008) 4317.
- [22] L. Wang, M. Zhang, X. Wang, W. Liu, *Mater. Res. Bull.* 43 (2008) 2220.
- [23] C. Wang, M.Y. Peng, L.Y. Yang, X. Hu, N. Da, D.P. Chen, C.S. Zhu, J.R. Qiu, *J. Rare Earths* 24 (2006) 754.
- [24] Y. Dong, J. Xu, G.Q. Zhou, G. Zhao, M.J. Jie, L.Y. Yang, L.B. Su, J.R. Qiu, W.W. Feng, L.H. Lin, *Opt. Lett.* 14 (2006) 1899.
- [25] Y. Dong, J. Xu, G.G. Zhao, C.F. Yan, G.Q. Zhou, L.B. Su, L.Y. Yang, J.R. Qiu, L.H. Lin, X.Y. Liang, R.X. Li, Z.Z. Xu, Q.S. Ren, *Opt. Mater.* 31 (2006) 2175.
- [26] M.J. Weber, *J. Appl. Phys.* 44 (1973) 3205.
- [27] Y. Liu, Y.B. Zhao, H.J. Luo, Z.S. Wu, Z.J. Zhang, *J. Nanopart. Res.* 13 (2011) 2041.
- [28] K. Klier, P. Novák, A.C. Miller, J.A. Spirko, M.K. Hatalis, *J. Phys. Chem. Solids* 70 (2009) 1302.
- [29] C. Dujardin, C. Pedrini, N. Garnier, A.N. Belsky, K. Lebbou, J.M. Ko, T. Fukuda, *Opt. Mater.* 16 (2001) 69.
- [30] R. Adhikari, G. Gyawali, S.H. Cho, R. Narro-García, T. Sekino, S.W. Lee, *J. Solid State Chem.* 209 (2014) 74.